Supporting Information

Construction and mechanistic understanding of high-performance all-air-processed perovskite solar cells via mixed-cation engineering

Wenyuan Zhang[a], Lang He[b], Yuanchao Li[a], Dongyan Tang[a], Xin Li[a,*], Limin Chang[c,*]

[a]*MIIT Key Laboratory of Critical Materials Technology for New Energy Conversion and Storage, School of Chemistry and Chemical Engineering, State Key Lab of Urban Water Resource and Environment, Harbin Institute of Technology, Harbin 150090, China.*

[b]*The Institute of Technological Sciences, Wuhan University, Wuhan, 430072, China.*

[c]*Key Laboratory of Preparation and Applications of Environmental Friendly Material of the Ministry of Education & College of Chemistry, Jilin Normal University, Changchun 130103, China.*

*Corresponding Author: Xin Li; Limin Chang

E-mail address: lixin@hit.edu.cn (X. Li); changlimin2139@163.com (L. Chang)

1. Experimental

1.1 Reagents and materials

The SnO_2 aqueous colloidal dispersion (tin (IV) oxide, 15 wt % in H_2O colloidal dispersion) was purchased from Alfa Aesar. Lead iodide (PbI_2), Methylammonium iodide (CH_3NH_3I), formamidinium iodide (FAI) and 2, 2′, 7, 7′-tetrakis-(N, N-di-4-methoxyphenylamino)-9, 9′ spirobifluorene (Spiro-OMeTAD) were obtained from Xi'an Polymer Light Technology Corp. 4-tert-butypyridine and lithium bis(trifluoromethanesulfonyl)imide (Li-TFSI) were purchased from Kanto. Dimethylformamide (DMF, purity > 99 %), and dimethyl sulfoxide (DMSO, purity > 99 %) were purchased from Youxuan Trade. All other anhydrous solvents were purchased from Aladdin. All chemicals and solvents were used without any further purification.

1.2 Fabrication of SnO_2 film

The SnO_2 aqueous colloidal dispersion is diluted with deionized water in a volume ratio of 1:5 and then was stirred overnight at room temperature as well as sonicated for 15 min. After that, the SnO_2 solution was coated onto the substrates by spin-coating at 500 rpm. for 3 s, 5000 rpm. for 40 s, then, the compact SnO_2 layer was annealed at 100 °C for 20 min. This process was repeated there times and then the SnO_2 film was annealed at 100 °C for 1 h in atmospheric environment without humidity control.

1.3 Solar cells fabrication

Fluorine-doped tin oxide (FTO) substrates were ultrasonically cleaned in detergent solution, deionized water, ethyl alcohol and acetone for 30 min respectively, followed by an UV-ozone treatment for 15 min. The $CH_3NH_3PbI_3$ perovskite precursor solutions were prepared by dissolving PbI_2(1.2 M), different proportions of MAI (1.2 M) and FAI (1.2 M) in mixed solvent of DMF and DMSO (4:1 volume/volume). The perovskite precursor solution was deposited onto the prepared FTO/SnO_2 substrate by a typical one-step anti-solvent method. Where the precursor solution was spin-coated on the substrates at a low speed of 500 rpm for 3 s followed by a high speed of 3000 rpm for 50 s, and 400 mL of anti-solvent (EA and ether) was dripped at a constant speed on the substrate. The film was heated at 70 °C for 5 min and 120 °C for 10 min to obtain a mirror-like brown-black perovskite film. After cooling to room temperature, the hole transport layer solution containing 80 mg of Spiro-OMeTAD, 28.5 μL 4-tert-butypyridine, 17.5 μL Li-TFSI (520 mg of Li-TFSI in 1 mL of acetonitrile) all dissolved in 1 mL chlorobenzene was deposited by spin-coating at 3000 rpm for 20 s. Finally, about 60 nm thick Au counter electrode was deposited via vacuum thermal evaporation at rate of 1.0 Å s^{-1}. The 0.09 cm^2 active area of the PSCs was determined through a non-reflective metal mask. All processes were operated in air (the average temperature was 25 °C, average relative humidity was 37.5 %).

1.4 Characterization and measurement

X-ray diffraction (XRD) pattern was obtained by a Panalytical Empyrean X-ray diffractometer with a Cu Kα radiation (λ=1.540598 Å) at a scan rate of 10° min^{-1}. The morphology and cross-section SEM image of the samples were observed by the Cold

Field Emission scanning electron microscopy (SEM, Carl Zeiss, Supra55). Atomic force microscopy (AFM) was obtained by Bruker Dimension FastScan Scanning Probe Microscope (SPM) using the tapping mode. Optical microscope (OM) image of the samples were observed by Olympus BX61. The UV-Visible spectrometer (TU1901, Beijing Purkinje General Instrument Co., Ltd) was used to measure the UV-vis absorption spectrum of different films. Steady-state photoluminescence (PL) and time-resolved photoluminescence (TRPL) spectroscopies measurements were conducted on V2.7 fluorescence spectrometer from HORIBA, the excitation wavelength is 532 nm. the reduced density gradient (RDG) function and the ρ (r) function was simulated through density functional theory (DFT) at B3LYP function with 6-31G (d, p) basis set, which was performed with the Gaussian 09 program package.

Photocurrent densitye-voltage (*J-V*) curves, open circuit voltage decay (OCVD) curves and the electron trap-state density tests were measured with an electrochemical workstation (VersaSTAT 3, Ametek, USA) and a 150 W xenon lamp class ABB solar simulator (94021A, Newport, USA) as standardized by a standard Si solar cell (1218, Newport, USA), where PSC devices were illuminated under AM1.5 radiation (1 sun conditions, 100 mW cm^{-2}). The sweep rate was 0.2 V s^{-1}. 50 devices were fabricated and measured independently to obtain the statistical histograms of PCEs. The incident photon-to-electron conversion efficiency (IPCE) was measured using the Crowntech solar cell quantum efficiency measurement system (QTest Station 500AD, USA). Electrochemical impedance spectroscopy (EIS) was obtained by the electrochemical workstation with a bias of -1.10 V, the process was in the dark state and the frequency

range was 0.1-100 KHz. The EIS data was fitted by the software of ZView2 according to the equivalent circuit model. All the measurements were performed in air condition and the devices were stored without any encapsulation.

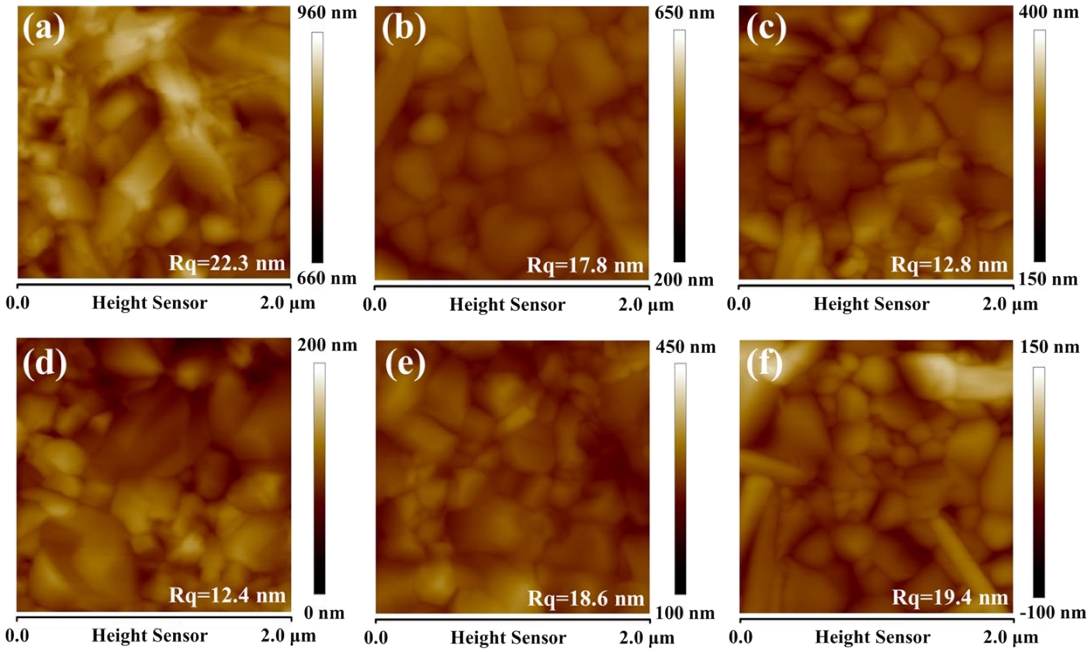

Fig. S1. AFM height images of (A) $MAPbI_3$ film and $FA_xMA_{1-x}PbI_3$ perovskite films with different FA ratios: (b) x=0.1; (c) x=0.2; (d) x=0.3; (e) x=0.4; (f) x=0.5. Corresponding Rq roughness are also displayed therein.

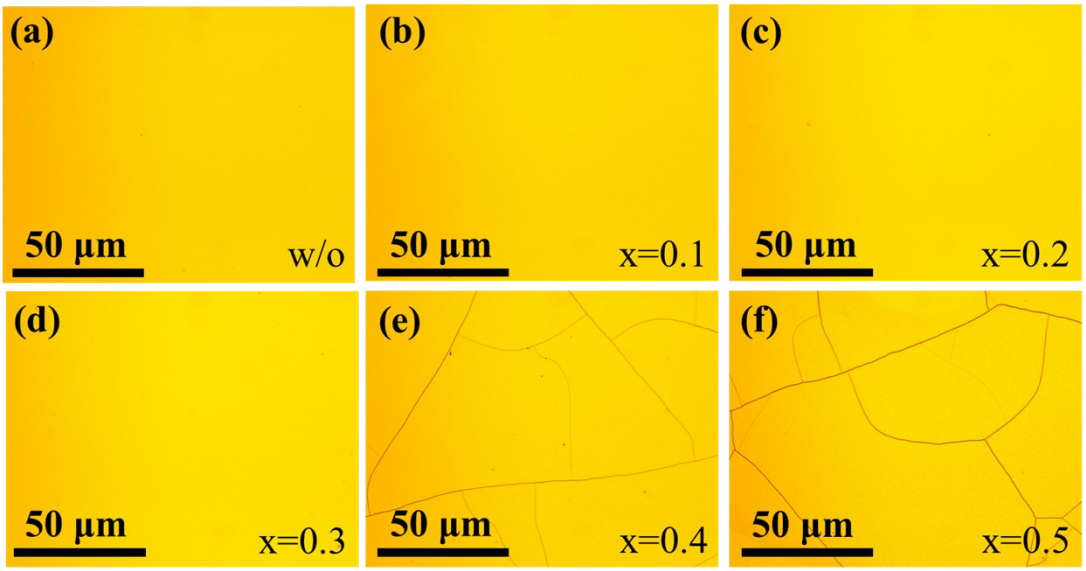

Fig. S2. OM images of (A) $MAPbI_3$ film and $FA_xMA_{1-x}PbI_3$ perovskite films with different FA ratios: (b) x=0.1; (c) x=0.2; (d) x=0.3; (e) x=0.4; (f) x=0.5.

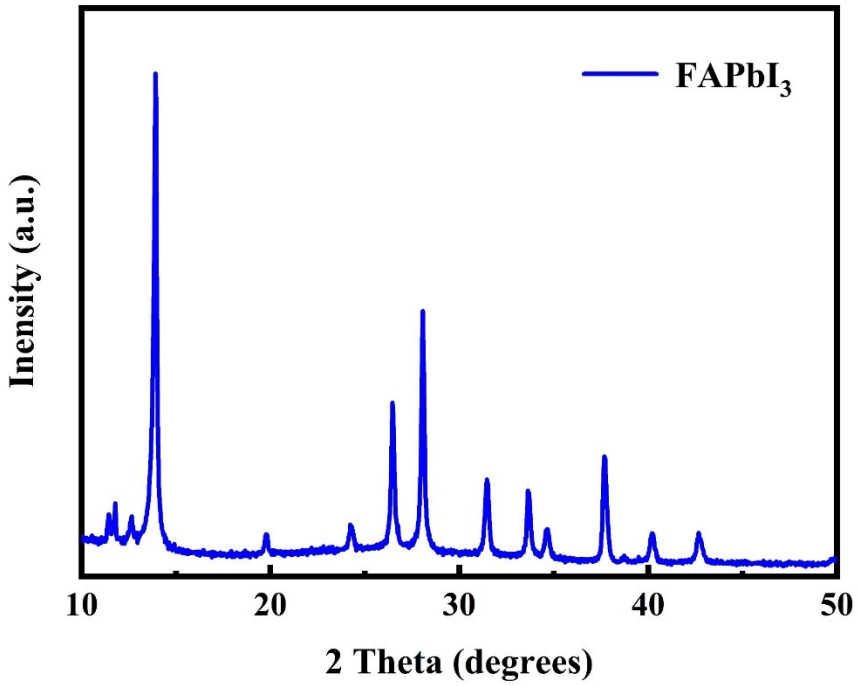

Fig. S3. XRD characterization of $FAPbI_3$ film.

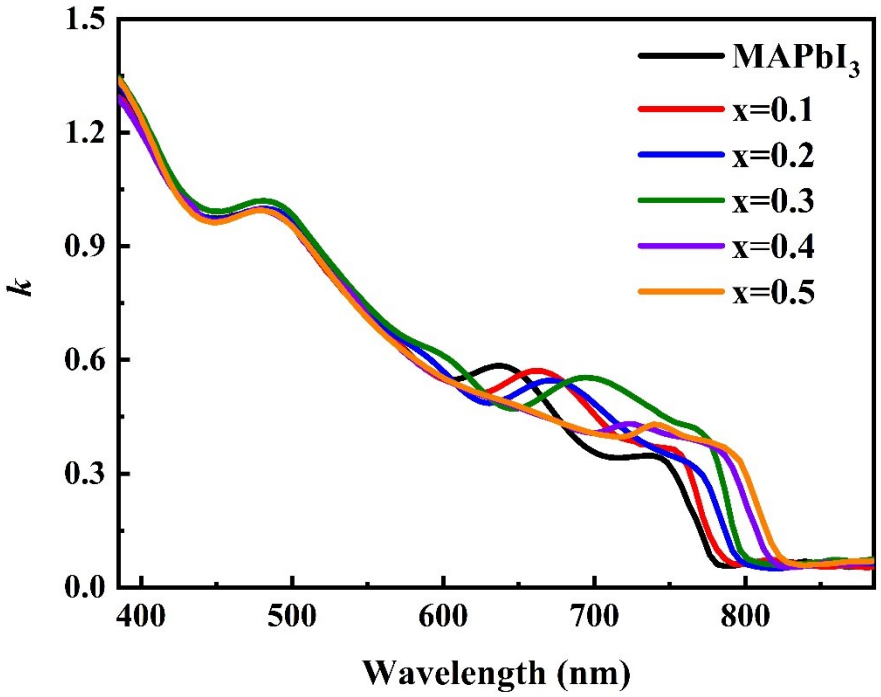

Fig. S4. The extinction coefficient (*k*) spectra of $MAPbI_3$ and $FA_xMA_{1-x}PbI_3$ films with different FA ratios.

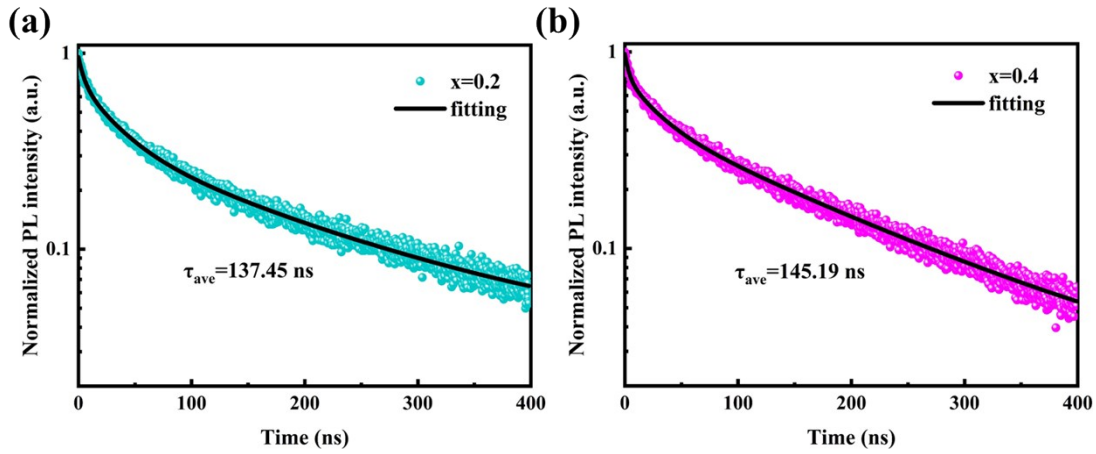

Fig. S5. TRPL spectra of $FA_xMA_{1-x}PbI_3$ films with (a) x=0.2 and (b) x=0.4 on glass substrates.

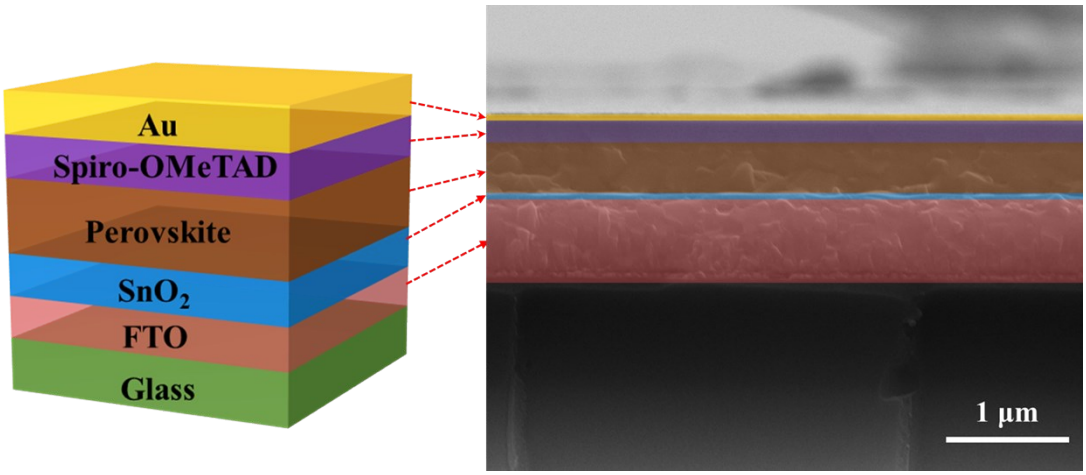

Fig. S6. The schematic diagram and cross-sectional SEM image of the PSCs device.

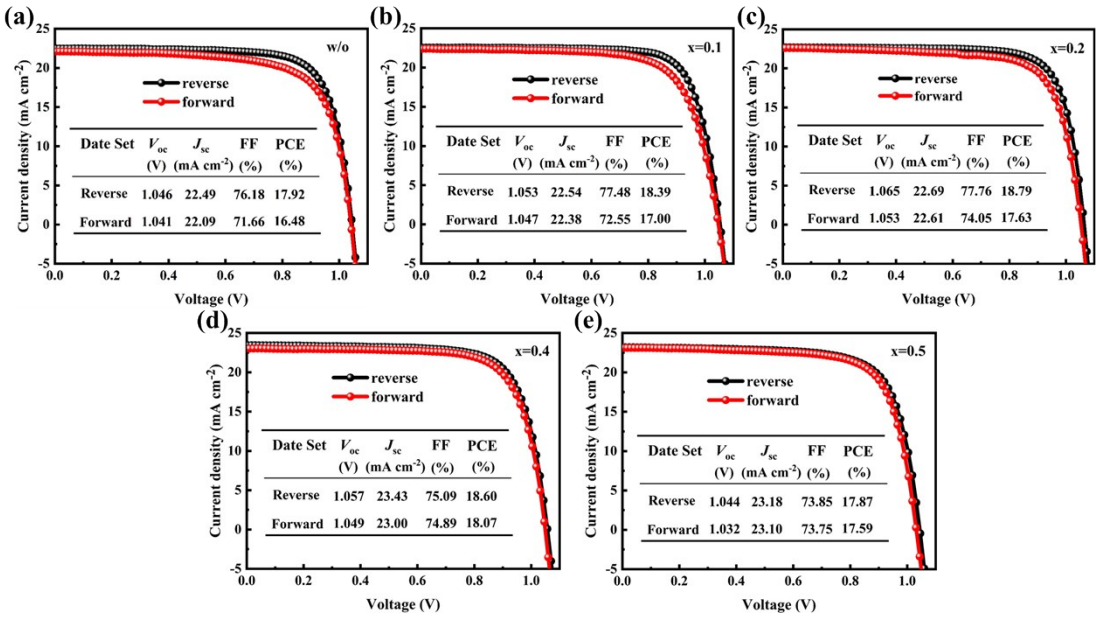

Fig. S7. *J-V* curves of the champion (a) $MAPbI_3$-device and $FA_xMA_{1-x}PbI_3$ with different FA ratios device (b) x=0.1; (c) x=0.2; (d) x=0.4; (e) x=0.5 under forward and reverse scan.

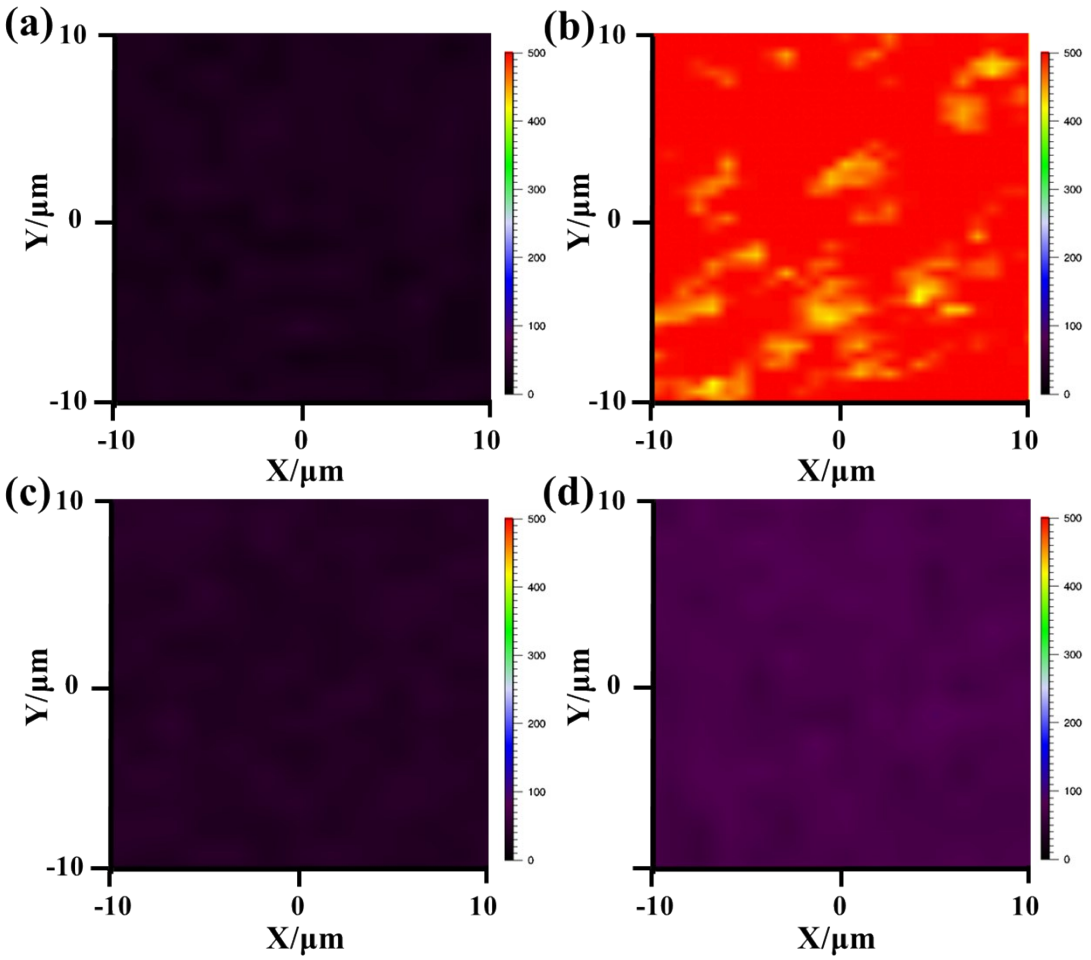

Fig. S8. Raman intensity mapping of $MAPbI_3$ film heated at 100 ℃ and 45 % RH for (a) 0 h and (b) 27 h. Raman intensity mapping of $FA_{0.3}MA_{0.7}PbI_3$ film heated at 100 ℃ and 37.5 % average RH for (a) 0 h and (b) 27 h. The excitation light source is a 15 mW 532 nm CW laser and the scanning step is 0.5 μm.

Table S1. Summary of references about high-performing all-air-processed PSCs.

Year	V_{oc} (V)	J_{sc} (mA cm^{-2})	FF (%)	PCE (%)	Ref.
2020	1.120	22.57	79.00	19.92	Ref. 1
2020	1.080	21.50	84.00	19.50	Ref. 2
2020	1.10	22.82	76.67	19.20	Ref. 3
2019	1.120	22.50	75.90	19.10	Ref. 4
2020	1.115	21.44	74.58	17.83	Ref. 5
2020	1.030	21.72	79.53	17.77	Ref. 6
2021	1.056	22.55	74.38	17.71	Ref. 7
2020	1.088	21.87	71.53	17.02	Ref. 8
2019	1.110	23.16	78.01	20.05	Ref. 9
2018	1.140	23.60	77.00	20.80	Ref. 10

Table S2 Fitting parameters by using a three-component exponential decay function for TRPL spectra of $MAPbI_3$ film and $FA_xMA_{1-x}PbI_3$ perovskite films with different FA^+ ratios.

Type	A_1	τ_1 (ns)	A_2	τ_2 (ns)	A_3	τ_3 (ns)	τ_{ave} (ns)
$MAPbI_3$	0.51	5.69	0.46	22.86	0.18	135.83	94.48
x=0.1	0.71	3.95	0.36	24.91	0.21	166.31	129.41
x=0.2	0.91	4.89	0.45	31.59	0.34	173.05	137.45
x=0.3	0.93	1.89	0.18	20.02	0.45	217.46	189.10
x=0.4	0.31	3.61	0.31	26.53	0.45	160.68	145.19
x=0.5	0.37	5.58	0.31	30.44	0.40	162.08	141.57

Table S3 ZView2 fitting parameters obtained from the EIS data of the champion devices based on $MAPbI_3$ film and $FA_xMA_{1-x}PbI_3$ films with different FA ratios.

Type	R_s (Ω)	R_{ct} (Ω)	C (F)
$MAPbI_3$	22.90	101.60	$7.65E^{-8}$
x=0.1	21.34	93.93	$7.42E^{-8}$
x=0.2	21.70	71.40	$7.01E^{-8}$
x=0.3	21.65	55.50	$7.85E^{-8}$
x=0.4	21.80	80.10	$7.91E^{-8}$
x=0.5	21.80	143.50	$7.45E^{-8}$

Table S4. The stability parameters of PSCs without any encapsulation tested under ambient condition (the average temperature was 25 °C, average relative humidity was 37.5 %).

Perovskite	Parameters	0 days	5 days	10 days	20 days	45 days	65 days	90 days
$MAPbI_3$	J_{sc}(mA cm^{-2})	22.49	22.25	22.10	21.85	21.73	21.17	20.38
	V_{oc} (V)	1.046	1.038	1.024	1.012	1.008	0.993	0.97
	FF(%)	76.15	75.02	73.12	71.95	71.57	70.74	70.01
	PCE(%)	17.92	17.33	16.55	15.91	15.68	14.87	13.84
$FA_{0.3}MA_{0.7}PbI_3$	J_{sc}(mA cm^{-2})	22.86	22.83	22.80	22.77	22.28	22.02	21.45
	V_{oc} (V)	1.085	1.076	1.072	1.057	1.052	1.040	1.029
	FF(%)	78.62	78.28	77.08	76.21	76.20	75.75	75.18
	PCE(%)	19.50	19.23	18.84	18.32	17.85	17.35	16.61

References:

[Ref. 1] R. Xia, X. X. Gao, Y. Zhang, N. Drigo, V. I. E. Queloz, F. F. Tirani, R. Scopelliti, Z. Huang, X. Fang, S. Kinge, Z. Fei, C. Roldán Carmona, M. K. Nazeeruddin and P. J. Dyson, *Adv. Mater.*, 2020, **32**, 2003801.

[Ref. 2] K. Zhang, Z. Wang, G. Wang, J. Wang, Y. Li, W. Qian, S. Zheng, S. Xiao and S. Yang, *Nat. Commun.*, 2020, **11**, 1006.

[Ref. 3] W. Zhang, L. He, D. Tang and X. Li, *Solar RRL*, 2020, **4**, 2000376.

[Ref. 4] G. Wang, C. Liu, W. Kong, H. Chen, D. Li, A. Amini, B. Xu and C. Cheng, *Solar RRL*, 2019, **3**, 1800324.

[Ref. 5] W. Zhang, Y. Li, X. Liu, D. Tang, X. Li and X. Yuan, *Chem. Eng. J.*, 2020, **379**, 122298.

[Ref. 6] Y. Deng, S. Li, X. Li and R. Wang, *Sol. Energ. Mat. Sol. C.*, 2020, **215**, 110594.

[Ref. 7] W. Zhang, X. Zheng, Y. Li, L. He and X. Li, *Electrochim. Acta*, 2021, **371**, 137812.

[Ref. 8] Y. Guo, X. Li, L. Kang, C. Cheng, X. He, X. Liu, J. Liu, Y. Li and C. Dong, *ACS App. Energy Mater.*, 2020, **3**, 9856-9865.

[Ref. 9] L. Chao, Y. Xia, B. Li, G. Xing, Y. Chen and W. Huang, *Chem*, 2019, **5**, 995-1006.

[Ref. 10] T. Singh and T. Miyasaka, *Adv. Energy Mater.*, 2018, **8**, 1700677.